Photoionization of Metastable O^+ Ions: Experiment and Theory

A. M. Covington, A. Aguilar, I. R. Covington, M. Gharaibeh, C. A. Shirley, and R. A. Phaneuf
Department of Physics, MS 220, University of Nevada, Reno, Nevada 89557-0058

I. Álvarez, C. Cisneros, and G. Hinojosa
Centro de Ciencias Físicas, Universidad Nacional Autónoma de México, Apartado Postal 6-96, Cuernavaca 62131, México

J. D. Bozek, I. Dominguez, M. M. Sant'Anna,* and A. S. Schlachter
Advanced Light Source, Lawrence Berkeley National Laboratory, MS 7-100, Berkeley, California 94720

N. Berrah
Department of Physics, Western Michigan University, Kalamazoo, Michigan 49008-5151

S. N. Nahar
Department of Astronomy, Ohio State University, 174 W. 18th Avenue, Columbus, Ohio 43210

B. M. McLaughlin†
Institute for Theoretical Atomic and Molecular Physics, Harvard Smithsonian Center for Astrophysics, 60 Garden Street, Cambridge, Massachusetts 2138
(Received 7 July 2001; published 27 November 2001)

High-resolution absolute experimental measurements and two independent theoretical calculations were performed for photoionization of O^+ ions from the $^2P^o$ and $^2D^o$ metastable levels and from the $^4S^o$ ground state in the photon energy range 30–35.5 eV. This is believed to be the first comparison of experiment and theory to be reported for photoionization from metastable states of ions. While there is correspondence between the predicted and measured positions and relative strengths of the resonances, the cross-section magnitudes and fine structure are sensitive to the choice of basis states.

DOI: 10.1103/PhysRevLett.87.243002 PACS numbers: 32.80.Fb

Although the interaction of photons with ionized matter is critically important to our understanding of both astrophysical and laboratory plasmas, experiments to critically test theory have only recently become possible with the advent of third-generation synchrotron light sources of exceptional brightness. In this Letter, the first high-resolution absolute measurements for photoionization of a metastable ion are compared to two new theoretical calculations representative of the current state-of-the-art.

Oxygen is an important constituent in terrestrial and stellar atmospheres, where it is prevalent in atomic and molecular forms, both neutral and ionized. Metastable states of O^+ are produced by photoionization in the F region of the ionosphere [1] and are known to strongly influence the chemistry of the thermosphere [2]. The $^2P^o$ and $^2D^o$ metastable levels of O^+ have mean lifetimes of 14 s and 1.3 h, respectively [3], and are significantly populated relative to the $^4S^o$ ground state by electron impact [4]. Metastable O^+ ions are therefore abundant in laboratory discharges, ion sources, and beams.

The Opacity Project (OP) [5] is an extensive international collaboration to calculate and compile a database of collisional and radiative properties of all ionization stages of the first ten elements of the periodic table. The first experimental benchmark for photoionization of an ion in the OP database was the recent measurement for C^+ reported by Kjeldsen *et al.* [6]. The cross-section data for all ionization stages of oxygen in the OP database (called TOPbase) [7] have been updated by improved *R*-matrix calculations, where results are reported from the ground-state of O^+ [8,9], but not from the metastable levels. O^+ is isoelectronic with nitrogen, for which photoionization from the metastable levels has been studied theoretically [10]. In the present investigation, high-resolution absolute cross-section measurements are compared to two independent theoretical calculations for photoionization of O^+ from its $^4S^o$ ground state and from the $^2P^o$ and $^2D^o$ metastable levels.

The theoretical calculations were performed using the *R*-matrix method [11]. In the close-coupling approximation the core ion is represented by an *N*-electron system, and the total wave function expansion, $\Psi(E)$, of the $(N+1)$-electron system for any symmetry $SL\pi$ is expressed as

$$\Psi(E) = A \sum_i \chi_i \theta_i + \sum_j c_j \Phi_j , \qquad (1)$$

where A is the antisymmetrization operator, χ_i is the core wave function in a specific state $S_i L_i \pi_i$, and θ_i is the wave function for the $(N+1)$th electron in a channel labeled as $S_i L_i \pi_i k_i^2 \ell_i (SL\pi)$; k_i^2 is its incident kinetic energy. Φ_j's are the correlation functions of the $(N+1)$-electron

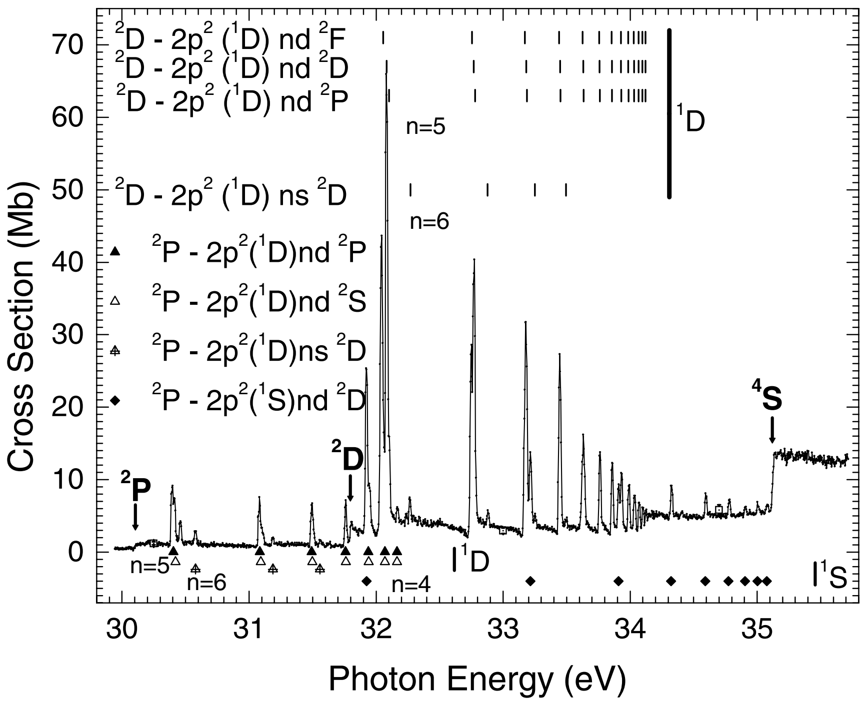

FIG. 1. Experimental cross section for photoionization of an admixture of 57% metastable and 43% ground-state O^+ as a function of photon energy in the range 30–35.5 eV. The nominal energy resolution is 17 meV. Threshold energies for photoionization from the $^2P^o$, $^2D^o$, and $^4S^o$ levels are indicated by vertical arrows. Rydberg series of resonances corresponding to $2p \rightarrow ns$ and $2p \rightarrow nd$ excitations to autoionizing levels from the metastable levels $^2P^o$ (triangles and diamonds) and $^2D^o$ (vertical lines) are identified. Absolute measurements are indicated by open squares at 30.25, 33.0, and 34.7 eV.

system that account for short-range correlation and the orthogonality between the continuum and the bound orbitals. $\Psi(E)$ is a bound $(N + 1)$-electron wave function when the energy $E < 0$ with all channels closed, and a free or continuum wave function when $E > 0$ with some or all continuum channels open.

In the first R-matrix calculation (A), cross sections for the three terms of the ground configuration $2s^2 2p^3(^4S^o, ^2D^o, ^2P^o)$ were obtained from the close-coupling approximation. Multiconfiguration expansions were employed for the twelve core O^{2+} states, including orbitals up to $3s$, with configurations of the form $2s^2 2p^2$, $2s2p^3$, $2s^2 2p3s$, and $2p^4$ [9]. The $3p$, $3d$, $4s$, and $4p$ orbitals used were correlated, allowing one to represent states, such as $2s^2 2p3s(^3P^o)$, which are important in photoionization because they correspond to strong dipole-allowed transitions in the core and enhance the background cross sections. All possible channels with the free electron angular momentum, $l \leq 9$, are considered, which generates all prominent resonances in the respective cross sections via channel couplings.

In the second R-matrix calculation (B), twenty-six states of the O^{2+} target were retained in the close-coupling calculations for the $^4S^o$ ground state and the $^2D^o$ and $^2P^o$ metastable states. Orbitals were included up to $4d$ [12]. Again, all the states were represented by multiconfiguration interaction wave functions and the R-matrix calculations were performed with forty continuum functions and a boundary radius of 13.6 Bohr radii. The calculations were performed in LS coupling with scattering wave functions generated by allowing all possible two-electron promotions out of the base $2s^2 2p^3$ configuration of O^+ into the orbital set employed. The outer region scattering problem was then solved using a fine energy mesh of 1.36 meV between thresholds in order to delineate the fine resonance structure in the respective photoionization cross sections.

The experiments were carried out on undulator beam line 10.0.1 at the Advanced Light Source using a newly developed ion-photon-beam end station. The photoion-yield spectroscopic technique using synchrotron radiation was pioneered by Lyon *et al.* [13] and applied recently by Kjeldsen *et al.* [6]. An energy-selected photon beam was merged over a path length of 29 cm with a highly collimated 6 keV O^+ beam produced in a hot-filament discharge ion source. Two-dimensional intensity distributions of both beams were measured by rotating-wire beam profile monitors installed just upstream and downstream of the interaction region, and by a translating-slit scanner in the middle of the region. A downstream analyzing magnet separated the O^{2+} products from the parent O^+ beam. A spherical electrostatic deflector directed the O^{2+} products onto a biased stainless-steel plate, from which secondary electrons were detected by a microsphere-plate electron multiplier and counted. The absolute efficiency of the photoion detector (0.210 ± 0.005) was determined by measuring the photoion current with an averaging subfemtoampere meter and comparing it to the measured count rate. The photon beam was mechanically chopped to separate photoions from O^{2+} ions produced by stripping collisions of O^+ with residual gas in the ultrahigh vacuum system. The photon energy and resolution were selected by a precision grating monochromator. The undulator gap in the 1.9 GeV electron synchrotron was set to maximize the photon intensity at each energy. The photon flux was recorded by a calibrated silicon x-ray photodiode, and was typically $(2-3) \times 10^{13}$ photons/sec at a nominal energy resolution of 20 meV.

Since the discharge in the ion source produces O^+ in both the ground and metastable states, and the lifetimes of the metastable states are much longer than the ion flight time in the apparatus, the measured photoion yields are proportional to a sum of the photoionization cross sections weighted by the population fractions of each component. The $^4S^o$ ground-state fraction was determined *in situ* by measuring the attenuation of the O^+ beam passing through a gas cell containing N_2 gas. Since the total cross section for electron capture by ground-state $O^+(^4S^o)$ from N_2 at 4 keV is 0.38 times that for metastable $^2P^o$ or $^2D^o$ [14], the ground-state fraction was determined by fitting a sum of exponentials to the transmitted O^+ current as a function of N_2 pressure. The ratio of the intercepts of the two decay components at zero gas-cell pressure yields a ground-state fraction of 0.43 ± 0.02. The electron capture cross sections for the two metastable components are too similar to be distinguishable by this method; only their sum of 0.57 ± 0.02 could be determined. A $^2P^o$ fraction of 0.15 ± 0.04 was estimated from the ratio of the measured absolute cross section times the $^2P^o$ fraction at a photon energy just above the $^2P^o$ ionization threshold to the theoretical $^2P^o$ photoionization cross section. This leads to an estimate for the $^2D^o$ fraction of 0.42 ± 0.05. These values were used to compare the results of the theoretical calculations to the measurements.

The measured photoionization cross section in the photon energy range 30–35.5 eV is presented in Fig. 1. The data represent a linear combination of the products of the photoionization cross section times the state fraction for the metastable and ground levels. Steps corresponding to the ionization thresholds [15] for $^2P^o$, $^2D^o$, and $^4S^o$ levels are evident at 30.10, 31.80, and 35.12 eV, respectively. The uncertainties in the absolute cross section and energy scale are estimated to be $\pm 16\%$ and ± 0.005 eV, respectively. The Rydberg series of resonances corresponding to $2p \rightarrow ns$ and $2p \rightarrow nd$ excitations to autoionizing levels from the $^2P^o$ and $^2D^o$ metastable levels are identified, along with their series limits, and, together with the three threshold steps, account for all of the observed features. The line shapes for the Rydberg series corresponding to $2p \rightarrow nd$ excitation from the $^2D^o$ state indicate strong interference between the direct and resonant photoionization channels.

The absolute experimental data are compared in Fig. 2 to theoretical calculations A and B, which have been convoluted with a Gaussian energy distribution with a FWHM of 17 meV to correspond to the measurements. To facilitate the comparison, the energy scales of the calculations have been offset by less than 1% so that the ionization thresholds for the $^2P^o$, $^2D^o$, and $^4S^o$ levels correspond to reference values [15], and the theoretical cross sections have been multiplied by the estimated $^2P^o$, $^2D^o$, and $^4S^o$ fractions in the experimental O^+ beam. The energy differences result from the numbers of terms and configurations used to represent the wave functions. While there is correspondence between the positions and relative strengths of the resonances in both cases, calculation B, which employed a finer energy mesh, more closely reproduces the measured resonance strengths. The experimental cross section for nonresonant photoionization just above the $^4S^o$ threshold (35.12 eV) is nearly double that predicted by both calculations, and does not clearly show the predicted resonance structure. Since the strong resonance feature near 32.75 eV corresponds only to excitation from the $^2D^o$ metastable state, it was selected for measurement at higher resolution. Figure 3 presents a comparison of photoion-yield measurements made at resolutions of 17 and 5 meV with the calculations (convoluted with 5 meV FWHM Gaussian). Theory A predicts the resonance positions more accurately since it used observed core rather than calculated threshold energies, such that the Rydberg series of resonances converge to the observed thresholds. However, theory B

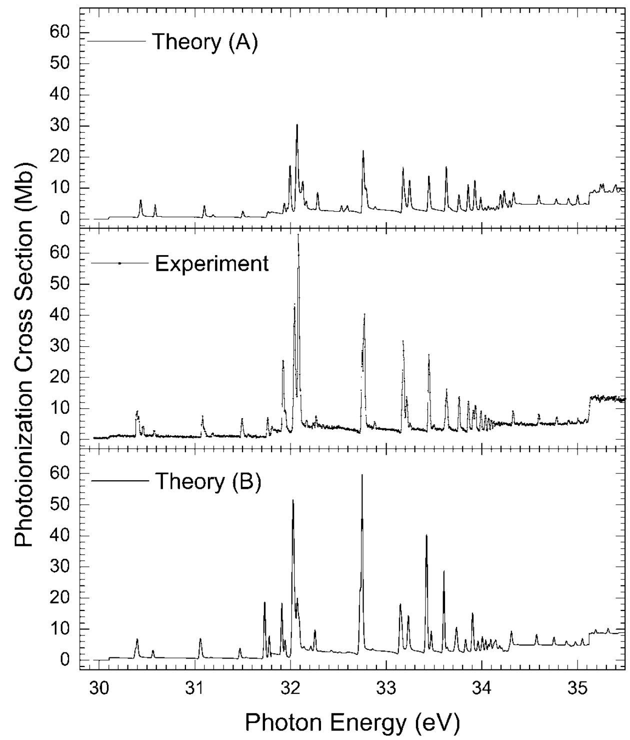

FIG. 2. Comparison of absolute photoionization measurements with theoretical calculations A and B. The calculated cross sections have been convoluted with a 17 meV FWHM Gaussian distribution, and their relative energy scales have been adjusted slightly to correspond to the standard reference values for the $^2P^o$, $^2D^o$, and $^4S^o$ ionization thresholds. The theoretical cross sections for each initial level have been multipled by the experimental fractions (0.15, 0.42, and 0.43, repectively), and summed.

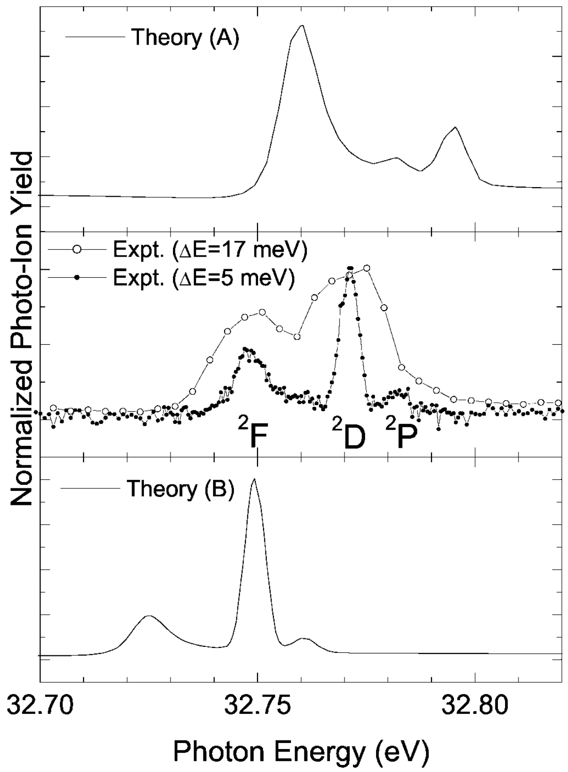

FIG. 3. High-resolution measurement of the resonance feature near 32.75 eV, corresponding to $2p \rightarrow 6d$ excitation from the $^2D^o$ state to the autoionizing states indicated. Data for $\Delta E = 17$ meV (open circles) and $\Delta E = 5$ meV (solid circles) are compared to theoretical calculations A and B, where the latter have been convoluted with a Gaussian with FWHM of 5 meV.

reproduces the relative intensities and widths better than theory A, as discussed above, mainly because of a finer energy mesh to resolve the resonances. Small differences are introduced due to differences in the wave functions in the two calculations.

In summary, high-resolution absolute photoion-yield spectroscopy using third-generation synchrotron radiation sources provides a powerful probe of the electronic structure of ions, not only in their ground state but also in metastable states. State-of-the-art theoretical methods for calculating photoionization of O^+ are successful in accounting for the main features of the photoionization process, and for predicting the cross section for photoionization from different initial states. However, the predicted resonance structure associated with the photoexcitation of autoionizing states is sensitive to the choice of basis functions.

The experimental work was supported in part by the DOE Divisions of Chemical Sciences, Geosciences and Biosciences, and Materials Sciences, by the DOE Facilities Initiative, by Nevada DOE/EPSCoR, by CONACyT and DGAPA (Mexico), and by CNPq (Brazil). The theoretical work was supported in part by NSF, by the Ohio Supercomputer Center, by ITAMP/Harvard-Smithsonian, and by EPSRC (UK).

*Present address: Pontifícia Universidade Católica do Rio de Janeiro, Rio de Janeiro 22452-970, Brazil.

†Present address: Department of Applied Mathematics and Theoretical Physics, The Queens University, Belfast BT7 1NN, United Kingdom.

[1] R. R. Meier, Space Sci. Rev. **58**, 1 (1991); S. S. Carr, R. J. Niciejewski, and T. L. Killeen, Geophys. Res. Lett. **20**, 2035 (1993); D. J. Melendez-Alvira, R. R. Meier, J. M. Picone, P. D. Feldman, and B. M. McLaughlin, J. Geophys. Res. **104**, 14 901 (1999).

[2] P. G. Richards, M. P. Hickey, and D. G. Torr, Geophys. Res. Lett. **21**, 657 (1994).

[3] W. L. Wiese, J. R. Fuhr, and T. M. Deters, in *Atomic Transition Probabilities of Carbon, Nitrogen and Oxygen: A Critical Data Compilation,* Journal of Physical and Chemical Reference Data No. 7 (AIP, New York, 1996).

[4] C. S. Enos, A. R. Lee, and A. G. Brenton, J. Phys. B **25**, 4021 (1992).

[5] M. J. Seaton, J. Phys. B **20**, 6363 (1987).

[6] H. Kjeldsen, F. Folkmann, H. Knudsen, M. S. Rasmusssen, J. B. West, and T. Andersen, Astrophys. J. **524**, L143 (1999).

[7] W. Cunto, C. Mendoza, F. Ochsenbein, and C. J. Zeippen, Astron. Astrophys. **275**, L5 (1993).

[8] V. M. Burke, D. J. Lennon, and M. J. Seaton, Mon. Not. R. Astron. Soc. **236**, 353 (1989).

[9] S. N. Nahar, Phys. Rev. A **58**, 3766 (1998).

[10] C. J. Zeippen, M. Le Dourneuf, and Vo Ky Lan, J. Phys. B **13**, 3763 (1980); K. L. Bell, K. A. Berrington, and C. A. Ramsbottom, J. Phys. B **25**, 1209 (1992); K. L. Bell and A. E. Kingston, Adv. At. Mol. Phys. **32**, 1 (1994).

[11] M. J. Seaton, J. Phys. B **20**, 6363 (1987); K. A. Berrington, P. G. Burke, K. Butler, M. J. Seaton, P. J. Storey, K. T. Taylor, and Yu. Yan, J. Phys. B **20**, 6379 (1987); P. G. Burke and K. A. Berrington, *Atomic and Molecular Processes: An R-Matrix Approach* (IOP, Bristol, UK, 1993).

[12] K. M. Aggarwal and A. Hibbert, J. Phys. B **24**, 3445 (1991).

[13] I. C. Lyon, B. Peart, J. B. West, and K. Dolder, J. Phys. B **19**, 4137 (1986).

[14] B. G. Lindsay, R. L. Merrill, H. C. Straub, K. A. Smith, and R. F. Stebbings, Phys. Rev. A **57**, 331 (1998).

[15] W. C. Martin, J. Sugar, and A. Musgrove, NIST Standard Reference Database Number 78, U.S. Department of Commerce, 1999.